123

A Note on Saltwater Intrusion in Coastal Aquifers

MOHSEN, M. SHERIF and VIJAY P. SINGH
Department of Civil Engineering, Lousiana State University, Baton Rouge, LA 70803-6405, U.S.A.

ABDELWAHAB M. AMER
Irrigation and Hydraulics Department, Faculty of Engineering, Cairo University, Giza, Egypt

Abstract. Transport of contaminants in aquifers has received considerable attention over the past few years. In coastal aquifers, a dispersion zone between saline water and fresh water exists where the flow of water and transport of salt ions are coupled. The flow pattern of two miscible fluids of different unit weights is characterized by the cyclic flow at the shore boundary. The width of the dispersion zone may be considerable, with the sharp interface assumption leading to erroneous results. A finite element model was applied to two prepublished problems for purposes of obtaining a better understanding of the saline water intrusion phenomenon. The effect of lowering the piezometric head due to excessive pumping was investigated. Physical parameters were extracted from the studies conducted by Kawatani and Rouve and Stoessinger, and comparison with their results was made.

Resumé. Pendant les dernières quelques années, le transport des contaminants dans les aquifères a reçu une attention considerable. Aux aquifères de la côte, il existe des zones où l'eau salé et l'eau douce se dispersent quand le flux de l'eau et le transport des ions du sel s'unissent. Le patron de flux [flow pattern] des fluides miscibles qui ont des différents unités de poids est characterisé par le flux cyclique au bord de la côte la largeur de la region de dispersion est considerable, et les suppositions de 'l'interface tranchante' [sharp interface] peut conduire a des faux résultats. Pour mieux comprendre le phénomène de l'instrusion de l'eau salé, le modèle des 'éléments limités' [finite element] a été appliqué dans deux problèmes déjà publiés. L'effet de l'abaissement piezométrique à cause du pompage excessif a été étudiés. Les paramètres physique ont été extraits des cas déjà étudiés, conduits par Rouven–Stoessinger et Kawatani, et la comparaisons avec leurs résultats a été fait.

1. Introduction

Population growth is one of the reasons for coastal regions being more densely populated. The resulting increase in the use of fresh groundwater in these regions tends to upset the long existing dynamic balance between fresh groundwater flow to oceans and saline ocean water.

A coastal aquifer can be threatened by saline water if it is in direct hydraulic contact with any saline water source. The density of saline water is greater than that of fresh water. Saline water migrates to the bottom of the aquifer and displaces the fresh water. A dispersion or transition zone exists where the flow of water and salt ions is coupled. The density of mixed water in the dispersion zone is

varied from the density of fresh water at the land side to that of seawater at the sea side. The flow of water is governed by the hydraulic gradient, while the transport of salt ions is under a concentration gradient. The width of the dispersion zone is a function of many parameters, such as aquifer type, aquifer geometry, medium properties, and the hydraulic gradient of fresh water.

Some investigations have been reported on the simulation of saltwater intrusion. Henry (1964) developed an analytical solution for the mass transport equation under steady-state conditions in idealized aquifers. Pinder and Cooper (1970) applied the method of characteristics to solve the convective-dispersion equation with a constant dispersion coefficient. Segol and Pinder (1976) applied the finite-element method to solve the same equation, taking into account the velocity-dependent dispersion coefficient. Sa da Costa and Wilson (1979), amongst others, also applied the finite-element method and a good discussion of the numerical methods used to solve the convective-dispersion equation is given by Huyakorn and Pinder (1983).

Kawatani (1980) solved the equation of motion for saturated flow in porous media for pressure, assuming the local change of liquid density, due to change in saltwater concentration, to be very small. While solving the transport equation, instability problems were encountered. To avoid these problems, he took constant dispersion coefficients. Cyclic flow appeared at the sea side to prevent the seawater from intruding deeply into the aquifer.

Rouve and Stoessinger (1980) simulated the movement of the saltwater interface in the Madras aquifer in south India using a numerical model based on a finite-element discretization technique. They established a functional equivalent of the differential equation to solve the density-dependent velocity field with the help of Legendre transformation. They utilized the formulation given by Meissner (1973). The Rouven–Stoessinger model did not exhibit any cyclic flow at the shore boundary.

This paper presents a numerical model for saltwater intrusion and flow pattern in coastal aquifers. The model is based on Galerkin's finite-element technique and local linearization of nonlinear terms, and uses an iterative procedure until convergence is achieved. The dispersion coefficients are taken to be velocity-dependent. The model is applied to two problems studied by Kawatani (1980) and Rouve and Stoessinger (1980). Equi-concentration and equi-potential lines are constructed for each case. Unlike the Rouven–Stoessinger model, cyclic flow is found near the seaside. The effect of lowering the piezometric head at the land side is also investigated.

2. Governing Equations

The governing equations describing saltwater intrusion in coastal aquifers for steady-state conditions are:

(1) *The mass balance equation for the fluid*:

$$\nabla \cdot \rho_q = 0 , \tag{1}$$

where ρ is the fluid density (kg/m^3), and $\mathbf{q}$ is the specific discharge (m/sec).

(2) *The mass balance equation for the dissolved salt or the hydrodynamic equation*:

$$n \, \nabla \cdot (D_h \cdot \nabla C) - \nabla \cdot \mathbf{q} \, C = 0 \, , \tag{2}$$

where n is porosity (dimensionless), C is concentration (kg/m^3), and D_h is the hydrodynamic dispersion coefficient (L^{2}T^{-1}) which can be expressed as (Bear, 1979)

$$D_{xx} = \alpha_L \, \frac{V_x^2}{|V|} + \alpha_T \, \frac{V_z^2}{|V|} + D^* \, ,$$

$$D_{zz} = \alpha_T \, \frac{V_x^2}{|V|} + \alpha_L \, \frac{V_z^2}{|V|} + D^* \, , \tag{3}$$

$$D_{xz} = D_{zx} = (\alpha_L \, \alpha_T) \, \frac{V_x V_z}{|V|} \, ,$$

where α_L and α_T are longitudinal and transverse dispersivities (L), V_x and V_z are pore velocities in x and z directions (LT^{-1}), $|V|$ is the resultant pore velocity (LT^{-1}), and D^* is molecular diffusion (L^{2}T^{-1}).

(3) *Darcy's equation for groundwater flow*:

$$\mathbf{q} = - K \, (\nabla \psi + \rho_r \, \nabla z) \, , \tag{4}$$

where K is the coefficient of permeability (LT^{-1}), ψ is the equivalent freshwater head (L), and ρ_r is the relative density and is equal to $\rho/\rho_f - 1$ (dimensionless), with ρ_f being the freshwater density and equal to 1000 kg/m^3.

(4) *A constitutive equation relating fluid density to salt concentration*:

$$\rho = \rho_f + a \, (C - C_f) \, , \tag{5}$$

where a is a dimensionless constant equal to 0.7246, and C_f is the freshwater concentration which is considered to be 0.5 kg/m^3.

3. Boundary Conditions

Consider the idealized confined coastal aquifer as shown in Figure 1. The lateral boundary at the land side is located at a point where the concentration is equal to C_f. The pressure at this boundary is hydrostatic and equal to $\gamma_f h$, where γ_f is the specific weight of freshwater (kg/m^3), and h is the piezometric head (m). At the sea boundary, the normal concentration gradient is equal to zero in the segment where the fluid leaves the system (through the window). A window is defined as the segment at the sea boundary through which the fluid finds its way out of the aquifer to the sea. In the segment where the seawater enters into the
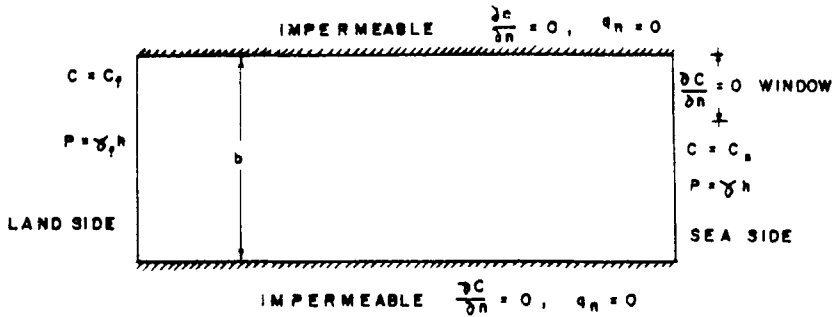
Fig. 1. Boundary conditions in an idealized confined coastal aquifer.

aquifer (below the window), the concentration is equal to seawater concentration C_s. Both upper and lower boundaries are impermeable, i.e. the normal flux for both the fluid and salt ions is equal to zero. Therefore, the boundary conditions can be written as follows:

For land side

$$\psi = \psi_L, \qquad C = C_f. \tag{6}$$

For sea side

$$\psi = \psi_x,$$

$$\frac{\partial C}{\partial n} = 0 \quad \text{over the window}, \tag{7}$$

$$C = C_s \quad \text{below the window}.$$

For upper and lower boundaries

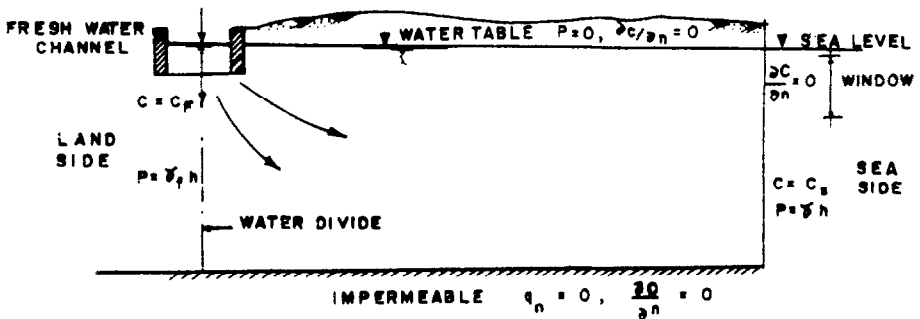$$q_n = 0, \qquad \frac{\partial C}{\partial n} = 0. \tag{8}$$

Fig. 2. Boundary conditions in an idealized unconfined coastal aquifer with fresh water channel at land side.

We now consider an idealized unconfined coastal aquifer with a freshwater channel at the land side creating a constant water table ridge above the sea level, as shown in Figure 2. The water table is considered as the upper boundary. The pressure along this boundary is atmospheric, and the normal concentration gradient is set as equal to zero. The other three boundary conditions will remain the same as in the case of confined aquifer.

4. Method of Solution

The hydrodynamic disperson equation is a nonlinear one. The velocity field and, hence, the dispersion coefficients, depend upon the concentration distribution. Pinder (1973), Grove (1977), Huyakorn and Pinder (1983), and Katopodes (1984) have indicated that Galerkin's procedure is well suited to solve mass transport problems.

Applying Galerkin's technique to the mass balance equation for flowing fluid and dissolved salt, we get

$$\int_v [N]^T (\nabla \cdot \rho \mathbf{q}) \; dv = 0, \tag{9}$$

$$\int_v [N]^T \{ n \nabla \cdot (D_h \cdot \nabla C) - \nabla \cdot \mathbf{q} C \} \; dv = 0, \tag{10}$$

where $[N] = [N_i \; N_j \; N_k]$ are the linear shape functions. Using Gauss' theorem and assuming unit thickness, Equations (9) and (10) can be written as

$$\int_{A^e} \frac{\partial [N]^T}{\partial x} (\rho q_x) \; dA^e + \int_{A^e} \frac{\partial [N]^T}{\partial z} (\rho q_z) \; dA^e$$

$$= \int_{L^e} [N]^T (\rho q_n) \; dL^e \tag{11}$$

and

$$\int_{A^e} \frac{\partial [N]^T}{\partial x} \left\{ n \left(D_{xx} \frac{\partial C}{\partial x} + D_{xz} \frac{\partial C}{\partial z} \right) - q_x C \right\} dA^e +$$

$$+ \int_{A^e} \frac{\partial [N]^T}{\partial z} \left\{ n \left(D_{xz} \frac{\partial C}{\partial x} + D_{zz} \frac{\partial C}{\partial z} \right) - q_z C \right\} dA^e$$

$$= \int_{L^e} [N]^T (n D_h \cdot \nabla C - q C_n) \; dL^e. \tag{12}$$

Equations (4), (5), (11) and (12) are combined into two nonlinear partial differential equations in only two variables, namely, the piezometric head and the concentration. These equations were solved by a two-step finite-element model. Initial estimate for the concentration at every point of the finite-element grid is given. Local and global coefficient matrices for the piezometric head $[K_\psi]$ as well as the vector of

known piezometric heads $[F_\psi]$ are constructed. The system of equations $[K_\psi][\psi]$ $= [F_\psi]$ is solved to find $[\psi]$ for all nodal points. The seaward boundary is updated by checking the directions of velocities at this boundary to locate the exact window length through which the mixed water leaves the system and the normal concentration gradient is set as equal to zero over the window. The hydrodynamic dispersion coefficients D_{xx}, D_{zz}, and D_{xz} are calculated, then local and global coefficient matrices for concentration $[K_C]$ as well as the vector $[F_C]$ of known coefficients are constructed. The system of equations $[K_C][C] = [F_C]$ is solved to find $[C]$ for all nodal points. The concentration is updated, then the previous steps are repeated until convergence is attained. Complete discussion on the mathematical derivation of the model, solution algorithm, and sensitivity analysis is given by Sherif (1987).

5. Model Application

The model was applied to two problems reported in the literature. The first problem is a hypothetical case and was investigated by Kawatani (1980). The second one was investigated by Rouve and Stoessinger (1980) for the Madras coastal aquifer.
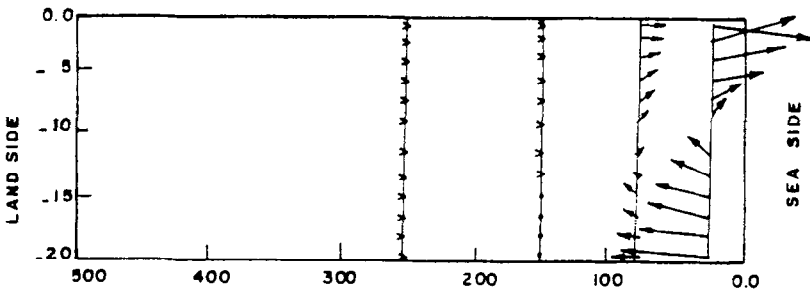
5.1. HYPOTHETICAL CASE

Kawatani (1980) considered the case of an unconfined coastal aquifer with a channel carrying fresh water at the land site, as shown in Figure 2. The water infiltration from the channel creates a constant water table above the sea level. If the infiltration from the channel is sufficient, a water divide will be formed somewhere beneath the channel, as shown in Figure 2. Kawatani considered the flow domain from the water divide at the land side to the shore boundary. To ensure the continuity of the velocity field, quadrilateral isoparametric elements were employed. Kawatani considered the case of a homogeneous anisotropic aquifer; the region of study was 500×200 m. The water table at the land side (fresh-water level in the channel) was 0.35 m above the sea level. He assumed the hydraulic conductivity in the x-direction, K_{xx}, to be 0.06 cm/min, and in z-direction, K_{zz}, to be 0.006 cm/min. An effective porosity of 0.25 was chosen over the entire flow domain. While solving the transport equation by finite difference or finite-element methods, instability occurs if the convective terms exceed a certain value related to the dispersion coefficients and the size of the finite elements, namely, when the local Peclet number is > 2.0 (Heinrich *et al.*, 1977). To avoid this instability problem, Kawatani assumed constant dispersion coefficients. He set D_{11}, D_{33} and D_{13} to be equal to 5, 0,5, and 0.05 cm²/min, respectively.

In this study, the same domain with the same hydraulic parameters and boundary conditions was considered to compare the results. The domain was represented by a uniform mesh with 1280 triangular elements with 697 nodes. To assess the stability of the numerical scheme of the model, the dispersion coefficients were taken to be velocity dependent as proposed by Bear (1979). The convergence criterion
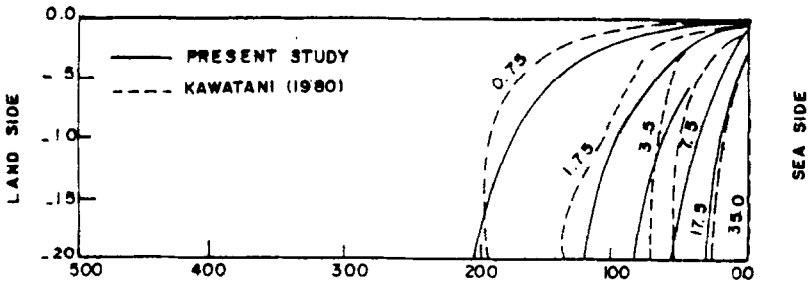
(a)

(b)
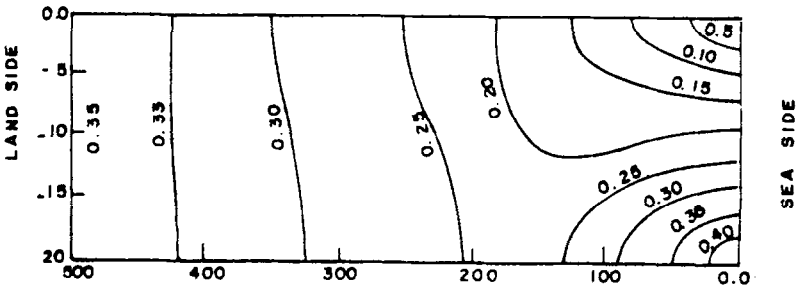
(c)

(a) COMPARISON BETWEEN EQUI - CONCENTRATION LINES
(b) FLOW PATTERN BY KAWATANI (1980)
(c) EQUI-POTENTIAL LINES FROM PRESENT STUDY

Fig. 3. Hypothetical case. (a) Comparison between equi-concentration lines; (b) flow pattern by Kawatani (1980); (c) equi-potential lines from present study.

ϵ was set as equal to 0.005.

A stable solution was found without any numerical oscillations. Convergence occurred in three iterations with a total cpu time of 3.64 sec. The code was run on a VM/370 IBM machine. Figure 3a compares the equi-concentration lines

obtained by the present model with those of Kawatani. A possible argument for the discrepancies between the two results is that different numerical schemes and different grid systems were used. Figure 3b shows the flow pattern in the aquifer obtained by Kawatani (1980). Figure 3c presents the equi-potential lines obtained from this study. Cyclic flow is evident at the sea boundary and also occurs when the velocity field at the sea boundary is rotational in character. The saltwater traverses away from the sea at the bottom of the aquifer and then circulates back into the sea through the upper segment of the boundary (or window). Cyclic flow was confirmed at the seaside, where the seawater intruded into the aquifer from the bottom of the aquifer. The seawater mixed with the freshwater and found its way back again to the sea, but with a lower concentration, through the window. This finding is also consistent with the investigations of Huyakorn and Taylor (1976), Anand and Pandit (1982), Pandit and Anand (1984), amongst others. Although Kawatani (1980) predicted the existence of cyclic flow from the velocity field, his model did not determine the shape of the equipotential lines in the aquifer and experienced some stability problems when solving the transport equation using velocity-dependent dispersion coefficients.
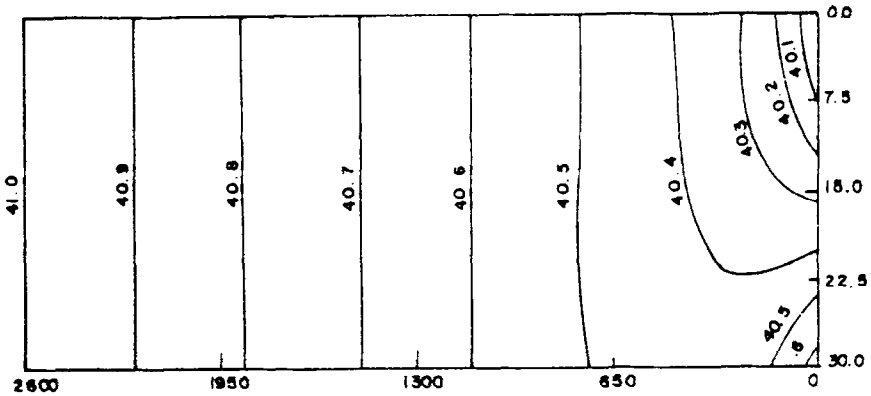
5.2. THE MADRAS AQUIFER

Rouve and Stoessinger (1980) applied a finite-element model to predict the saltwater intrusion in the Madras coastal aquifer in south India. Although the aquifer is a leaky heterogeneous one where significant flows occur through the overlying clay layers, they considered it to be a confined homogeneous one for purposes of simplicity. An average coefficient of permeability of 3×10^{-3} m/sec and a porosity of 0.35 were considered. Longitudinal and transverse dispersivities, α_L and α_T, were taken as 66.6 and 6.6 m, respectively. Molecular diffusion was set equal to 1×10^{-6} m²/sec. Because the thickness of the aquifer at the sea boundary is only 30 m, the limit up to which the influence of hydrodynamic dispersion can be expected is about 3 km.

The model was applied to the idealized representation of the Madras aquifer by Rouve and Stoessinger (1980). No observations about salinity distribution in the Madras aquifer were available. The results were compared with those of the Rouve–Stoessinger model, which considered the same study region (2600 × 30 m). The domain was represented by a uniform grid of 400 triangular elements and 246 nodes. The purpose of using a uniform grid system was to draw equi-concentration and equi-potential lines by using the available software system for data analysis called the GCONTOUR procedure. It should be noted that better discretization can be done by taking a finer grid system near the shoreline where cyclic flow exists and the concentration gradient is steeper. The convergence criterion ϵ was set as equal to 0.001. The piezometric head at the seaside was set to equal 40 m. To study the effect of lowering the piezometric head due to excessive pumping of the saltwater intrusion and flow pattern in the Madras aquifer, two different
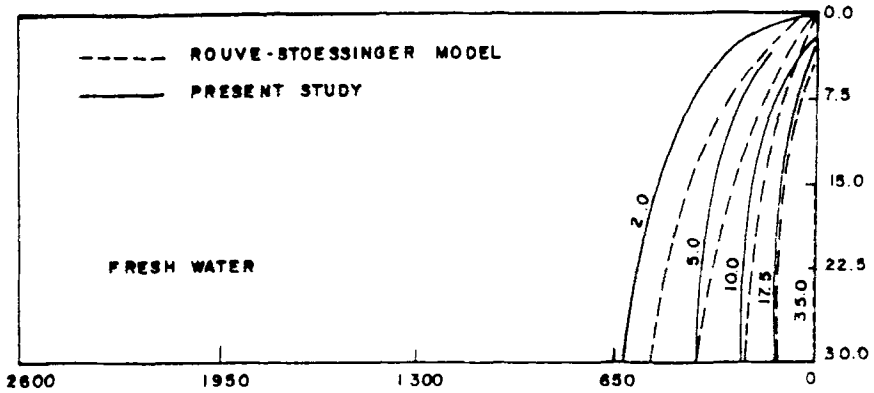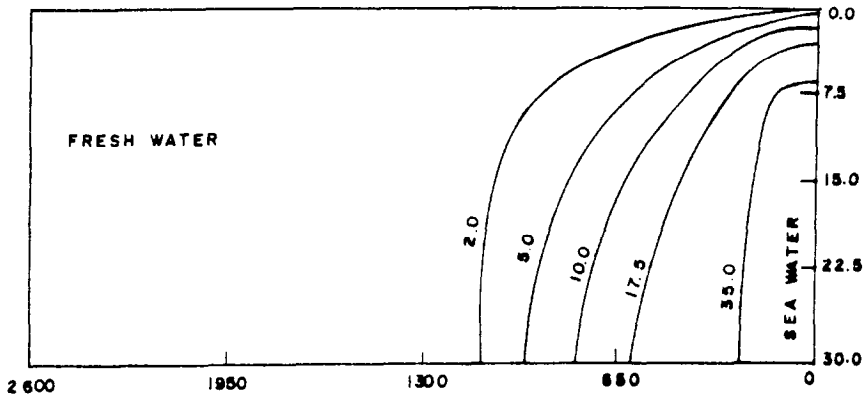
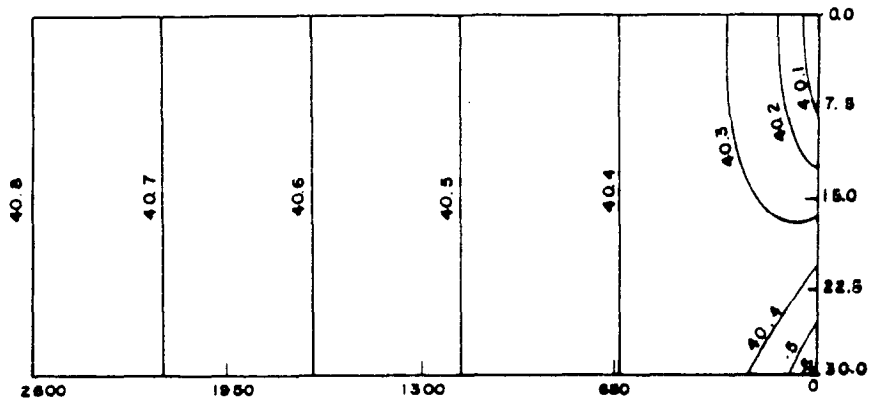Fig. 4. Equi-concentration and equi-potential lines in Madras aquifer (case one).

Table I. Concentration distribution in Madras aquifer (after Rouve and Stoessigner, 1980)

Y (m)	Shoreline, X (m)											
	0	50	120	220	440	600	850	1100	1400	1800	2200	2600
0	12.4	0	0	0	0	0	0	0	0	0	0	0
5	18.3	12.0	3.6	1.6	0.4	0.1	0	0	0	0	0	0
10	27.9	19.3	9.4	3.7	1.0	0.2	0.1	0	0	0	0	0
15	35.0	22.5	13.9	6.7	1.6	0.4	0.1	0	0	0	0	0
20	35.0	24.4	15.8	9.1	2.4	0.5	0.1	0	0	0	0	0
25	35.0	25.8	17.1	9.9	2.9	0.6	0.1	0	0	0	0	0
30	35.0	26.7	18.0	10.4	3.2	0.6	0.1	0	0	0	0	0

piezometric heads at the land side were considered. In the first case, the piezometric head at the land side was set to equal 41 m. Convergence was achieved within five iterations, with a total cpu time of 5.11 sec. The code was run on a VM1370 IBM machine.

Fig. 5. Equi-concentration and equi-potential lines in Madras aquifer (case two).

Table II.   Piezometric head in Madras aquifer (after Rouve and Stoessigner, 1980)

Y (m)	Shoreline, X (m)											
	0	50	120	220	440	600	850	1100	1400	1800	2200	2600
0	40.2	40.5	40.5	40.6	40.7	40.7	40.7	40.8	40.8	40.9	40.9	41.0
5	40.2	40.4	40.5	40.6	40.7	40.7	40.8	40.8	40.8	40.9	40.9	41.0
10	40.1	40.3	40.4	40.6	40.6	40.7	40.7	40.8	40.8	40.9	40.9	41.0
15	40.0	40.2	40.4	40.5	40.7	40.7	40.8	40.8	40.8	40.9	40.9	41.0
20	40.0	40.2	40.3	40.5	40.6	40.7	40.7	40.8	40.8	40.9	40.9	41.0
25	40.0	40.1	40.3	40.5	40.6	40.7	40.8	40.8	40.8	40.9	41.0	41.0
30	40.0	40.1	40.3	40.5	40.6	40.7	40.7	40.8	40.8	40.9	40.9	41.0

It was found that the width of the dispersion zone, which can be defined between equi-concentration lines 35 and 2, measured at the lower boundary was about 610 m. In the Rouve–Stoessinger model, the width of the dispersion zone measured at the same boundary was about 520 m, as shown in Figure 4a and also in Table I

Equi-concentration line 10 intruded inland 250 m from the sea boundary,while in the Rouve–Stoessinger model, it intruded 232 m.

Cyclic flow was predicted near the shoreline, as shown in Figure 4b, where saltwater found its way into the aquifer bottom, and again to the sea as a mixed water through the window. The Rouve–Stoessinger model did not exhibit any cyclic flow at the shore boundary as seen from Table II. Mixed water swept out to the see all over the sea boundary but under a different hydraulic gradient.

In the second case, the piezometric head at the land side was lower by 0.2 m than in the first case. Gonvergence was achieved within eight iterations, with a total cpu time of 7.96 sec. Seawater (equiconcentration in line 35) intruded inland to a distance of 260 m measured at the bottom boundary from the seaside. The width of the dispersion zone at the same boundary was about 840 m, as shown in Figure 5. Lowering the peizometric head allowed more saltwater to intrude the Madras aquifer through the lower part of the seaside boundary.

The piezometric head adjusted quickly and was nearly independent of the variation in the concentration. On the other hand, the concentration was very sensitive toany variation in the piezometric head.

6. Concluding Remarks

This paper applied a two-dimensional numerical model to simulate saltwater intrusion into coastal aquifers. The model used Galerkins finite-element technique with a linear base fuction. A clear and accurate determination of equi-concentration and equi-potential lines was made. The width of the dispersion zone is considerable (hundreds of meters) and cannot be ignored. Unlike the Kawatani model, no stability problems occurred in solving the transport equation using velocity-dependent dispersion coefficients. Lowering the piezometric head at the land side by 0.2 m enabled saltwater to intrude the bottom of the Madras aquifer to a distance of 260 m from the sea boundary.

Unlike the Rouve–Stoessinger model, cyclic flow was found near the shore boundary. Lowering the piezometric head at the land side emphasized the cyclic flow at the seaside. A comparison of results obtained in this study with those obtained by the Kawatani and Rouve–Stoessinger models was made. Although some investigators (Huyakorn and Taylor, 1976; Kawatani, 1980; Pandit and Anand, 1984) indicated the existence of cyclic flow at the shore boundary, none of them presented the shape of equi-potential lines. This study produced a clear and accurate picture not only of saltwater intrusion and the shape of equi-concentration lines, but also about the flow pattern and the shape of equi-potential lines in confined coastal aquifers.

References

Anand, S. G. and Pandit, A., 1982, Finite element solution for coupled groundwater flow and transport equations and transient conditions including the effect of the selected time step size, *Proc. 4th Internat. Conf. Finite Elements in Water Resources*, University of Hannover, Hannover, Germany.

Bear, J., 1979, *Hydraulics of Groundwater*, McGraw-Hill, New York.

Grove, D. B., 1977, The use of Galerkin finite-element methods to solve mass-transport equations, U.S. Geol. Survey Water Resources Investigations, 77–49.

Heinrich, J. C., Huyakorn, P. S., Mitchell, A. R., and Zienkiewicz, O. C., 1977, An upwind finite element scheme for two-dimensional convective transport equation, *Internat. J. Numer. Methods Engrg.* **11**.

Henry, H. R., 1964, Effect of dispersion on salt encroachment in Coastal aquifers, U.S. Geological Survey Water Supply Paper 1613-C.

Huyakorn, P. S. and Pinder, G. F., 1983, *Computational Methods in Subsurflace Flow*, Academic Press, New York.

Huyakorn, P. S. and Taylor, C., 1976, Finite element model for coupled groundwater flow and convective dispersion, *Proc. 1st Internat. Conf. Finite Elements in Water Resources*, Princeton, New Jersey.

Katapodes, N. D., 1984, A dissipative Galerkin scheme for open-channel flow, *J. Hydraul. Engrg.* **110**, 450–466.

Kawatani, T., 1980, Behavior of seawater intrusion in layered coastal aquifers, *Proc. 3rd Internat. Conf. Finite Element in Water Resources*, Univ. of Miss., Oxford, Miss.

Meissner, U., 1973, Die Berechnung ebener und Raumlicher Grund-u Sickerwasserstromungen mit verallgemeinerten variationsverfahren, Mitt. des SFB 79 f. Wasserforschung im Kustenbereich der TU Hannover, H.2.

Pandit, A. and Anand, S. G., 1984, Groundwater flow and mass transport by finite elements – a parametric study, *Proc. 5th Internat. Conf. Finite Elements in Water Resources*, University of Vermont.

Pinder, G. F., 1973, A Galerkin-finite element simulation of groundwater contamination on Long Island, *Water Resour. Res.* **9**(6), 1657–1669.

Pinder, G. F. and Cooper, H. H., 1970, A numerical technique for calculating the transient position of the saltwater front, *Water Resour. Res.* **6**(3), 875–882.

Rouve, G. and Stoessinger, W., 1980, Simulation of the transient position of the saltwater intrusion in the coastal aquifer near Madras coast, *Proc. 3rd Internat. Conf. Finite Elements in Water Resources*, Univ. of Miss., Oxford, Miss.

Sa da Costa, A. A. G. and Wilson, J. L., 1979, Numerical model of seawater intrusion in aquifers, MIT Report 247, Massachusetts Institute of Technology, Cambridge, Mass.

Segol, G. and Pinder, G. F., 1976, Transient simulation of waltwater intrusion in southeastern Florida, *Water Resour. Res.* **12**(1), 65–70.

Sherif, M. M., 1987, A Two-Dimensional Finite Element Model for Dispersion (2D-FED) in Coastal Aquifers, PhD thesis, Faculty of Engineering, Cairo University.

Stoessinger, W., 1979, Beschreibung der hydrodynamischen Dispersion mit der Methode der finiten Elemente am Beispiel der instationaren Interface zwischen Sub- und Salzwasser in Grundwasserleitern, Institut für Wasserbau und Wasserwirtschaft, Rheinisch-Westfalische Technische Hochschule Aachen, 28.